



Published in final edited form as:

Pract Radiat Oncol. 2020 ; 10(2): 104–111. doi:10.1016/j.prro.2019.10.016.

Electrocardiogram-Gated Computed Tomography with Coronary Angiography for Cardiac Substructure Delineation and Sparing in Patients with Mediastinal Lymphomas Treated with Radiation Therapy

Scott C. Lester, MD^{a,*}, Kekoa Taparra, PhD^{a,b}, Molly M. Petersen, MS^c, Ryan K. Funk, MD^a, Miran J. Blanchard, MD^a, Phillip M. Young, MD^d, Joerg Herrmann, MD^e, Ashley E. Hunzeker, CMD^a, Heather L. Schultz, CMD^a, Cynthia McCollough, PhD^a, Alexandria M. Tasson, MS^a, Shuai Leng, PhD^d, James A. Martenson, MD^a, Amanda J. Deisher, PhD^a, Thomas J. Whitaker, PhD^a, Eric E. Williamson, MD^d, Nadia N. Laack, MD^a

^aDepartment of Radiation Oncology, Mayo Clinic, Rochester, Minnesota

^bMayo Clinic Alix School of Medicine, Mayo Clinic, Rochester, Minnesota

^cDivision of Biomedical Statistics and Informatics, Mayo Clinic, Rochester, Minnesota

^dDepartment of Diagnostic Radiology, Mayo Clinic, Rochester, Minnesota

^eDepartment of Cardiology, Mayo Clinic, Rochester, Minnesota

Abstract

Purpose: (1) Demonstrate feasibility of electrocardiogram-gated computed tomography with coronary angiography (E-CTA) in treatment planning for mediastinal lymphoma and (2) assess whether inclusion of cardiac substructures in the radiation plan optimization (CSS optimization) results in increased cardiac substructure sparing.

Methods and Materials: Patients with mediastinal lymphomas requiring radiation therapy were prospectively enrolled in an observational study. Patients completed a treatment planning computed tomography scan and E-CTA in the deep inspiration breath hold position. Avoidance structures (eg, coronary arteries and cardiac valves) were created in systole and diastole and then merged into a single planning organ-at-risk volume based on a cardiac substructure contouring atlas. In the photon cohort, 2 volumetric modulated arc therapy plans were created per patient with and without CSS optimization. Dosimetric endpoints were compared.

Results: In the photon cohort, 7 patients were enrolled. For all 7 patients, the treating physician elected to use the CSS optimization plan. At the individual level, 2 patients had reductions of 10.8% and 16.2% of the right coronary artery receiving at least 15 Gy, and 1 had a reduction of 9.6% of the left anterior descending artery receiving 30 Gy. No other differences for coronary arteries were detected between 15 and 30 Gy. Conversely, 5 of 7 patients had >10% reductions

*Corresponding author: Scott C. Lester, MD; lester.scott@mayo.edu.

Disclosures: none.

Supplementary data

Supplementary material for this article can be found at <https://doi.org/10.1016/j.prro.2019.10.016>.

in dose between 15 to 30 Gy to at least 1 cardiac valve. The greatest reduction was 22.8% of the aortic valve receiving at least 30 Gy for 1 patient. At the cohort level, the maximum, mean, and 5-Gy increment analyses were nominally similar between planning techniques for all cardiac substructures and the lungs.

Conclusions: Cardiac substructure delineation using E-CTA was feasible, and inclusion in optimization led to modest improvements in sparing of radiosensitive cardiac substructures for some patients.

Introduction

Radiation continues to have a critical role for maximizing event-free survival in patients with Hodgkin and non-Hodgkin lymphomas.^{1,2} However, mediastinal radiation is well known to precipitate late cardiac effects.^{3,4} The consequences and risk of these effects are especially pronounced in patients with early-stage Hodgkin lymphoma (HL), who tend to be younger at diagnosis and experience high rates of long-term survival. Major advances have been made to minimize cardiac exposure to radiation. Successive clinical trials, institutional reports, and improvements in chemotherapy have led to substantive reductions in dose prescribed and field size.^{5–7} Technological advancements in diagnostic and therapeutic radiology have led to a significant expansion of tools to better target and modulate radiation delivery. Despite these advances, many patients still receive collateral radiation to cardiac structures that elevates their risk for late toxicity. Taken in context with the published finding that there is no minimal threshold for therapeutic radiation exposure to the heart,^{8,9} further advances are critical to maximize the therapeutic ratio for patients with mediastinal lymphomas.

The heart is most often considered a single structure for dosimetric purposes. This is likely a reflection that a conventional computed tomography (CT)–based radiation simulation provides limited detail for cardiac substructure identification and localization. However, late cardiac effects typically manifest as coronary artery disease, cardiomyopathy, and cardiovalvular disease, which suggests that substructure dose may drive specific forms of cardiac toxicity. This principle has been supported by the finding that coronary artery dose is more predictive of ischemic cardiac toxicity than whole-heart dose.¹⁰

Multiple imaging modalities have been used to outline cardiac substructures, including coronary angiography.¹¹ Cardiac-timed contrast administration allows optimal identification of the coronary arteries and cardiac valves. However, a particular challenge in cardiac substructure delineation is the multiple interdependent physiological forces that lead to continuous anatomic change and displacement. The heart and substructures are in constant oscillation within systole and diastole. Accurate localization of substructures for potential avoidance therefore depends on temporal resolution in addition to spatial resolution. Electrocardiogram-gated CT angiography (E-CTA) enables accurate visualization and delineation of substructures at the maximum and minimum displacements within the cardiac cycle.¹² Cardiac filling and emptying is also simultaneously affected by the effect of the respiratory cycle on intrathoracic pressure. Thus cardiac substructures need to be imaged throughout the respiratory cycle as well as the cardiac cycle or intrathoracic pressure

must be held constant by the use of deep inspiratory breath hold (DIBH). Recent efforts to quantify substructure motion have demonstrated ranges from 7 to 15 mm of movement when allowing for respiratory motion and ranges from 3 to 7 mm when controlling for respiratory motion.^{13,14}

We present our experience from a prospective clinical trial that incorporated E-CTA into radiation oncology clinical practice for treatment of mediastinal lymphomas and evaluate whether incorporation of cardiac substructures into the optimization process is feasible and leads to lower substructure doses when treating with volumetric modulated arc therapy (VMAT).

Methods and Materials

Patients

This trial was approved by the Mayo Clinic institutional review board. Patients between 7 and 65 years of age with biopsy-proven Hodgkin or non-Hodgkin lymphoma were prospectively enrolled when scheduled for radiation therapy. Exclusion criteria included pregnancy or severe renal insufficiency defined as a serum creatinine >1.9 mg/dL. Informed consent was obtained from all patients ≥18 years old and legal guardians. Informed assent was obtained from all patients <18 years old participating in this study. Clinical staging was based on the Lugano classification of the modified Ann Arbor staging.¹⁵ All patients underwent initial staging with FDG-18 positron emission tomography and CT (PET/CT).

Simulation

Immobilization was fabricated for each patient and customized under the direction of the treating physician at the time of simulation. All patients who were able to comply were initially imaged using a deep inspiration breath hold (DIBH) technique with real-time position management (RPM). A second identical scan was then completed with intravenous contrast timed for soft tissue and vessel enhancement. At a separate appointment, the patient resumed the treatment position using custom immobilization in the department of diagnostic radiology. A CT angiogram was acquired using iodinated contrast in the DIBH without the use of the RPM guidance. ECG gating was created using a retrospective algorithm that automatically reconstructs prespecified phases of the cardiac cycle. These images were then coregistered with the treatment-planning imaging.

Target and organ-at-risk delineation

A study-specific cardiac substructure contouring atlas was developed with input from a multidisciplinary team of experts in radiation oncology, medical physics, diagnostic radiology, and cardiology. This atlas is available online in the appendix and available for download. All contouring was completed on the standard, noncontrast CT scan produced from simulation. Target volumes were defined using involved site radiation therapy principles consistent with the contemporary standard.¹⁶ Standard organs at risk (OARs) were defined. Cardiac substructures including the left anterior descending artery, left circumflex artery, right coronary artery, aortic valve, pulmonic valve, mitral valve, tricuspid valve, and left ventricle were contoured on the systole and diastole scans separately. Each substructure

in the separate phases of the cardiac cycle was then combined to form a singular OAR. Additionally, the whole heart was contoured in systole, diastole, and then combined via the Boolean function into a single planning OAR volume.

Treatment-planning IMRT

Two IMRT plans were then designed using Eclipse planning software (Varian Medical Systems, Inc, Palo Alto, CA). The cardiac substructure-sparing (CSS) optimization plan used cardiac substructures in the optimization process. The non-CSS plan was optimized with the same target coverage normalization but did not include cardiac substructures in the optimization process and treated the heart as a single unit. In general, an initial attempt was made to limit coronary and valve structures to a maximum dose of 15 Gy. If the former could not be met with acceptable target coverage, a target constraint of mean dose of less than 15 Gy was used. Target coverage was not compromised to achieve either constraint. Both plans were then reviewed, and the selection of the optimal plan was solely at the discretion of the treating physician. For purposes of comparison, target coverage was normalized to 95%. However, for the plan actually delivered, coverage exceeding 95% of the target volume was permitted.

Dosimetric analysis

Doses to cardiac substructures, the whole heart, and the lungs were compared for VMAT plans optimized with and without cardiac substructures. Averaged maximum, mean, and 5-Gy increments were nominally compared between the CSS-optimized and standardly optimized plans. Additionally, individual differences of substructure doses greater than 10% per 5-Gy increment were identified and tabulated.

Results

Patient characteristics

Twenty-two patients consented to enrollment, of which 1 was excluded by trial criteria for absence of a documented pregnancy test. Of those, 7 patients were treated with VMAT, and the characteristics are summarized in Table 1. The median age of patients treated with VMAT was 30 years (range, 14–58 years). Two patients had primary mediastinal B cell lymphoma, 2 patients had diffuse large B cell lymphoma, and 3 patients had classical Hodgkin lymphoma. All patients were staged with PET/CT. Six patients had stage II disease, and 1 patient had stage IV. Before chemotherapy, 5 patients had disease greater than 15 cm in greatest diameter, and all had mediastinal masses of at least 5 cm in greatest diameter. All patients had disease extending at least to or below the left main coronary artery.

Treatment characteristics

Treatment characteristics are also summarized in Table 1. All patients were initially treated with anthracycline-based chemotherapy or immunochemotherapy as primary treatment ($n = 6$) or for refractory disease ($n = 1$) before referral for adjuvant radiation therapy. The patient with refractory disease was initially treated for HL with ABVD but was found to have persistent disease after 3 cycles. Therapy was escalated to BEACOPP, which also provided only a partial response. A repeat biopsy of the mediastinal mass demonstrated diffuse large

B cell lymphoma. This prompted a change in therapy to R-DHAP. After 2 cycles, a repeat PET/CT demonstrated local progression. The patient was then referred for radiation therapy. All patients were able to satisfactorily complete DIBH at simulation. Patients were treated with 21 Gy in 14 fractions (n = 1), 30 Gy in 15 fractions (n = 5), and 40 Gy in 20 fractions (n = 1). All 7 patients were treated with the plan optimized to spare cardiac substructures.

Individual patient dosimetry

The impact of including cardiac substructures on the aggregate dosimetric comparison above may not accurately reflect the impact on individual patients with variable target volumes and anatomy. We analyzed the difference in substructure dose by 5-Gy increments on a per-patient basis to further address this. A difference of 10% or more was considered potentially meaningful.

The patient achieving the largest dosimetric difference in coronary artery dose using CSS optimization had reductions of 28.6% and 15.2% of the volume of the left anterior descending artery receiving at least 10 Gy and 5 Gy respectively, and a 47.1% reduction in the volume of the circumflex receiving at least 5 Gy (Fig 1). Three patients experienced increases >10% in coronary artery dose with CSS optimization. For 1 of these patients, CSS optimization increased the volume of the left circumflex and left anterior descending arteries receiving at least 5 Gy by 13.2 and 24.3% respectively while simultaneously decreasing the volume receiving at least 15 Gy by 10.8%. Another experienced a 16.3% reduction in the volume of the right coronary artery receiving at least 15 Gy with a concordant increase of 12.3% in the volume receiving at least 10 Gy. No coronary artery volume was different by 10% or more for any patient in the dose ranges of 20 to 30 Gy, although the volume of the right coronary artery receiving at least 30 Gy was decreased by 9.6% in 1 patient.

Five of 7 patients had reductions in at least 1 cardiac valve parameter with CSS optimization. The greatest sparing was observed for the aortic valve, which was improved in 5 of 7 patients and unchanged for the other 2. The volume of the aortic valve receiving at least 30 Gy was reduced by 22.8% for 1 patient, and 4 patients had reductions between 11% and 63% of the volume of the aortic valve receiving at least 15 Gy. In the 15-to-30-Gy range, no valve was increased by more than 10% in any metric when using CSS optimization.

The mean heart dose was reduced using CSS optimization by 1.0, 0.8, and 0.4 Gy in 3 patients; increased by 0.3 Gy in 1 patient; and unchanged in the remaining 3 patients.

Doses to cardiac substructures

All 7 patients underwent prospective comparative assessment of VMAT plans generated with and without CSS optimization. Comparative cardiac substructure dose-volume histograms are displayed in Figure 2. There were no apparent clinically meaningful differences between mean or maximum substructure doses achieved with CSS and non-CSS optimization. The greatest difference in substructure dose between techniques was for the mean dose to the aortic valve (7.9 vs 13.0 Gy with and without CSS). However, this difference is unlikely to be clinically meaningful. Similar trends were appreciated for the pulmonary and tricuspid valves, but not for the mitral valve (38.1% vs 38.4%). When each

substructure was analyzed by 5-Gy increments, there were no apparent clinically meaningful differences (Tables E1–E5, available online at <https://doi.org/10.1016/j.prro.2019.10.016>).

Doses to heart and lungs

Comparative heart and lung dose-volume histograms are displayed in Figure 3. The primary purpose of investigating lung, whole-heart, and left ventricle dose was to ensure that attempting to avoid cardiac substructures did not result in additional dose deposits within these conventional structures. There were no apparent clinically meaningful differences between mean or maximum substructure doses achieved with CSS optimization and those without. The mean heart dose with and without CSS optimization was 10.02 Gy vs 10.31 Gy. When analyzed in 5-Gy increments, the percent of the heart receiving 15 Gy and 20 Gy was nominally lower when using CSS optimization (15 Gy: 24.3% vs 26.5%; 20 Gy: 17.8% vs 18.8%). There were no differences in lung or left ventricle dose between the techniques when analyzed by 5-Gy increments.

Discussion

External beam radiation therapy continues to have an important role in the treatment of mediastinal lymphomas. In an effort to maximally spare cardiac substructures with known toxicity from radiation exposure, we conducted a pilot study to evaluate the feasibility of incorporating ECG-gated CT scanning with coronary angiography into radiation therapy treatment planning and whether inclusion of cardiac substructures in the VMAT optimization provides clinically meaningful reductions in doses delivered to cardiac substructures.

Multiple challenges were overcome to streamline and optimize the process. Initially, fabrication of custom immobilization and standard simulation with DIBH was completed in the department of radiation oncology. Then the patient and radiation therapy team completed the E-CTA in the treatment position in the department of radiology at a separate appointment without the use of RPM guidance. This process was resource intensive and inconvenient for the patient and introduced potential sources of additional uncertainty. Because of these drawbacks, a Siemens SOMATOM Definition (AS Open RT, 64-slice configuration) with 0.33-second rotation time was installed within the radiation oncology department. Of note, this is still below the typical slice count used in standard ECG-gated CT scans for diagnostics purposes, which generally use CT scanners with 200 to 300 slice capability. We developed a department-specific protocol for completion of the E-CTA at the time of simulation. No patient was pretreated with beta blockers, as is often done to ensure a low heart rate at the time of scanning.¹⁷

After acquiring the planning CT and marking the isocenter on the patient, electronic leads are connected from the patient to the CT scanner to synchronize the scanner with the patient's heart rate. A single axial pre-monitoring slice 2 mm below the carina is obtained, and a region of interest is identified at the aortic root. Monitoring of this region of interest commences 7 seconds after contrast injection starts, and a limited-range (cardiac volume only) breath hold scan is triggered automatically when the HU threshold is met. A third full-range (same volume as the planning CT) scan is immediately performed to capture

the contrast between the thoracic vasculature and soft tissues for target volume delineation. After becoming familiar with the protocol, all 3 scans can be completed within 20 minutes.

For the overall cohort, the benefits of including cardiac substructures in the optimization were limited to modest reductions in the volume of the heart receiving at least 20 Gy. The lack of aggregate improvement is in part related to the high variability of the disease location and its anatomic relationship to the heart. It is also in part related to the inherent physical limitations of megavoltage photons. For some patients it is likely that a single heart contour is adequate for sparing of these as a collective, and additional granularity for optimization is unnecessary. Of the substructures analyzed, the aortic valve was the most likely structure to benefit from CSS optimization with photons. We found it difficult to spare substructures that were abutting or nearly abutting target volumes regardless of their inclusion in the optimization. The aortic valve is centrally located within the heart, which likely accounts for the increased sparing observed when including it in the optimization.

Strengths of this study include the ability of the treating physician to prospectively select the preferred plan, incorporation of state-of-the-art treatment techniques including involved site target volume delineation with VMAT and DIBH,¹⁸ and multidisciplinary-designed, study-specific cardiac substructure contouring atlas (Appendix E1, available online at <https://doi.org/10.1016/j.prro.2019.10.016>). The findings of this study are limited by our evolving understanding of the clinical effects of substructure dose. Although a relationship between dose and cardiac toxicity has been established for patients with Hodgkin lymphoma,⁹ it is not known whether the modest reductions seen in this study for some patients would translate into clinical benefit in the present highly conformal era. Additionally, although the enhanced resolution of cardiac substructures did not translate into dose reductions using VMAT at the cohort level, additional improvements in conformality can be achieved with proton therapy. To further explore this issue, we continued enrolling on this protocol as the Mayo Clinic Proton Therapy Center came online and have undertaken comparative planning with the described VMAT technique. Although this technology and workflow represent a potential technical advancement, it is important to note that there are inherent technical limitations. The position of the cardiac substructures was not verified with daily imaging during treatment or monitored intrafractionally. Changes in cardiac filling from alterations in volume status, heart rate, and immediate pretreatment activity level could all potentially degrade the daily reproducibility of substructure location. Additionally, patients in this series only completed 1 ECG-gated CT, and it is not known whether DIBH reliably facilitates a reproducible position for the cardiac substructures. Lastly, it must be mentioned that this is a resource-intensive approach to radiation planning, and contouring all cardiac substructures in each phase typically takes 1 to 2 hours.

Conclusions

Electrocardiogram-gated computed tomography with coronary angiography can be feasibly incorporated into radiation therapy workflow and allows for optimal identification of radiosensitive cardiac substructures throughout the cardiac cycle. Because of the variable anatomic relationship of target volumes to cardiac substructures, the benefit of incorporating

cardiac substructure delineation into radiation therapy planning was only observed at the individual level.

Supplementary Material

Refer to Web version on PubMed Central for supplementary material.

Sources of support:

The study was funded by the Mayo Clinic departments of cardiology, radiology, and radiation oncology. Dr Taparra was supported by the 2017 American Society for Radiation Oncology Minority Summer Fellowship Award.

References

1. André MPE, Girinsky T, Federico M, et al. Early positron emission tomography response–adapted treatment in stage I and II Hodgkin lymphoma: Final results of the randomized EORTC/LYSA/FIL H10 trial. *J Clin Oncol*. 2017;35:1786–1794. [PubMed: 28291393]
2. Olszewski AJ, Shrestha R, Castillo JJ. Treatment selection and outcomes in early-stage classical Hodgkin lymphoma: Analysis of the National Cancer Data Base. *J Clin Oncol*. 2015;33: 625–633. [PubMed: 25584010]
3. Stewart FA. Mechanisms and dose-response relationships for radiation-induced cardiovascular disease. *Ann ICRP*. 2012;41: 72–79. [PubMed: 23089006]
4. Aleman BM, van den Belt-Dusebout AW, De Bruin ML, et al. Late cardiotoxicity after treatment for Hodgkin lymphoma. *Blood*. 2007; 109:1878–1886. [PubMed: 17119114]
5. Specht L, Yahalom J, Illidge T, et al. Modern radiation therapy for Hodgkin lymphoma: Field and dose guidelines from the International Lymphoma Radiation Oncology Group (ILROG). *Int J Radiat Oncol Biol Phys*. 2014;89:854–862. [PubMed: 23790512]
6. Sasse S, Bröckelmann PJ, Goergen H, et al. Long-term follow-up of contemporary treatment in early stage Hodgkin lymphoma: Updated analyses of the German Hodgkin study group HD7, HD8, HD10, and HD11 trials. *J Clin Oncol*. 2017;35:1999–2007. [PubMed: 28418763]
7. Engert A, Plütschow A, Eich HT, et al. Reduced treatment intensity in patients with early stage Hodgkin's lymphoma. *N Engl J Med*. 2010;363:640–652. [PubMed: 20818855]
8. Darby SC, et al. Risk of ischemic heart disease in women after radiotherapy for breast cancer. *N Engl J Med*. 2013;368:987–998. [PubMed: 23484825]
9. van Nimwegen FA, Schaapveld M, Janus CP, et al. Cardiovascular disease after Hodgkin lymphoma treatment: 40-year disease risk. *JAMA Intern Med*. 2015;175:1007–1017. [PubMed: 25915855]
10. Hahn E, Jiang H, Ng A, et al. Late cardiac toxicity after mediastinal radiation therapy for Hodgkin lymphoma: Contributions of coronary artery and whole heart dose-volume variables to risk prediction. *Int J Radiat Oncol Biol Phys*. 2017;98:1116–1123. [PubMed: 28721895]
11. Duane F, Aznar MC, Bartlett F, et al. A cardiac contouring atlas for radiotherapy. *Radiother Oncol*. 2017;122:416–422. [PubMed: 28233564]
12. Sun Z, Ng KH. Prospective versus retrospective ECG-gated multi-slice CT coronary angiography: A systematic review of radiation dose and diagnostic accuracy. *Eur J Radiol*. 2012;81:e94–e100. [PubMed: 21316887]
13. Guzhva L, Flampouri S, Mendenhall NP, Morris CG, Hoppe BS. Intrafractional displacement of cardiac substructures among patients with mediastinal lymphoma or lung cancer. *Adv Radiat Oncol*. 2019;4:500–506. [PubMed: 31360806]
14. Kataria T, Bisht SS, Gupta D, et al. Quantification of coronary artery motion and internal risk volume from ECG gated radiotherapy planning scans. *Radiother Oncol*. 2016;121:59–63. [PubMed: 27641783]
15. Cheson BD, Fisher RI, Barrington SF, et al. Recommendations for initial evaluation, staging, and response assessment of Hodgkin and non-Hodgkin lymphoma: The Lugano classification. *J Clin Oncol*. 2014;32:3059–3067. [PubMed: 25113753]

16. Illidge T, Specht L, Yahalom J, et al. Modern radiation therapy for nodal non-Hodgkin lymphoma —target definition and dose guidelines from the International Lymphoma Radiation Oncology Group. *Int J Radiat Oncol Biol Phys.* 2014;89:49–58. [PubMed: 24725689]
17. Sabarudin A, Sun Z. Beta-blocker administration protocol for prospectively ECG-triggered coronary CT angiography. *World J Cardiol.* 2013;5:453–458. [PubMed: 24392189]
18. Petersen PM, Aznar MC, Berthelsen AK, et al. Prospective phase II trial of image guided radiotherapy in Hodgkin lymphoma: Benefit of deep inspiration breath-hold. *Acta Oncol.* 2015;54:60–66. [PubMed: 25025999]

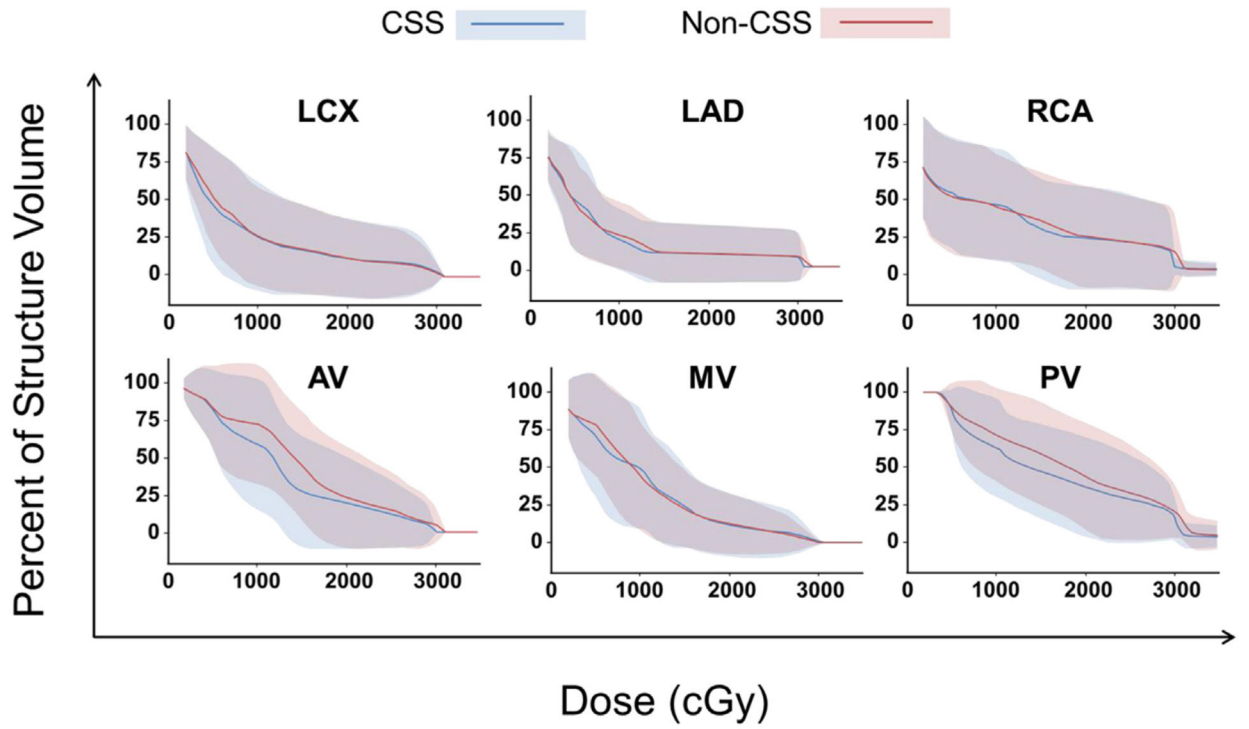


Figure 1. Comparative dose-volume histograms with doses achieved to each cardiac substructure with (blue) and without (red) cardiac substructures-sparing.

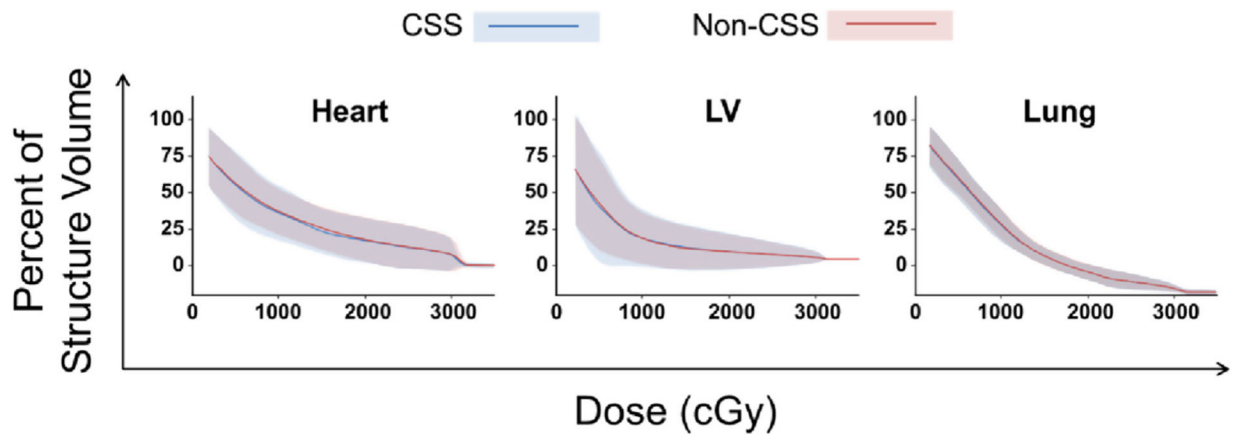


Figure 2.

Comparative dose-volume histograms with doses achieved with (blue) and without (red) cardiac substructures. No increase in critical normal thoracic organs at risk was observed by using cardiac substructures in the optimization.

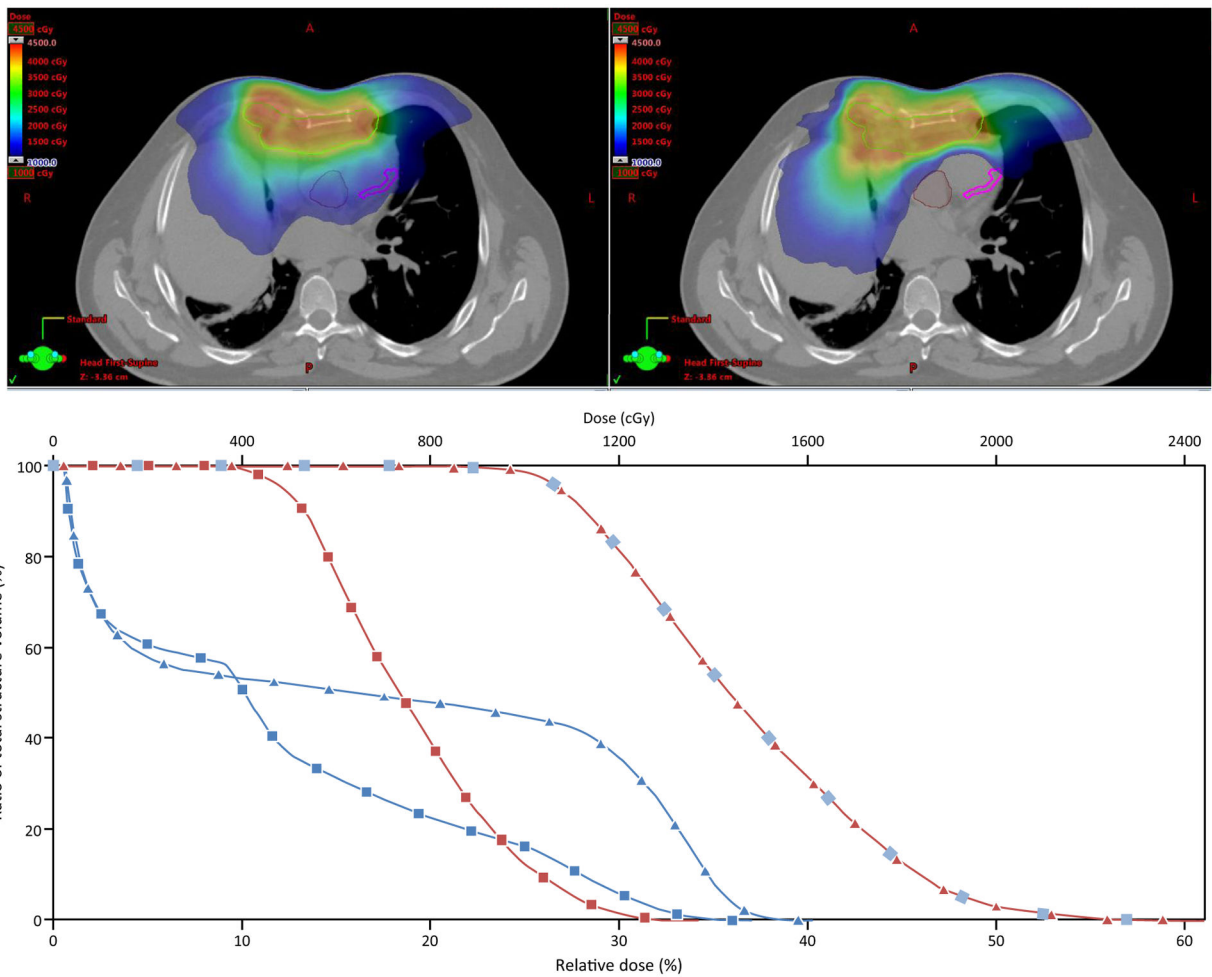


Figure 3. Dose reductions to the left anterior descending artery (pink) and aortic valve (brown) by including cardiac substructures in the optimization for patients receiving mediastinal radiation therapy, 40 Gy in 20 fractions, for a chemo-refractory diffuse large B-cell lymphoma. In the dose-volume histogram, the squares correspond with the cardiac substructure-sparing plan, and the triangles correspond with the noncardiac substructure-sparing plan.

Table 1

Patient and treatment characteristics

	N = 7
Age at Diagnosis	
Median years	30
Range	14–58
Lymphoma Type	
Hodgkin	3
Diffuse large B cell	2
Primary mediastinal B cell	2
Initial Stage	
II	6
IV	1
PET/CT used	7
Mediastinal Mass, cm	
5	7
15	5
Initial Therapy	
Chemo or immunochemotherapy	7
Lymphoma status at radiation	
Controlled	6
Refractory	1
Radiation Techniques Used	
VMAT with DIBH	7
Gy/fractions	
21/14	1
30/15	5
40/20	1

Abbreviations: CT = computed tomography; DIBH = deep inspiration breath hold; PET = positron emission tomography; VMAT = volumetric modulated arc therapy.